THE AMERICAN SOCIETY OF MECHANICAL ENGINEERS
345 E. 47 St., New York, N.Y. 10017

88-GT-190

Investigation into the Effect of Tip Clearance on Centrifugal Compressor Performance

JOOST J. BRASZ
United Technologies Carrier
Carrier Parkway
Syracuse, New York 13221

ABSTRACT

The axial clearance between the tip of the blades of an unshrouded impeller and its stationary shroud has been varied to study its effect on overall compressor performance. The compressor under investigation consisted of an inlet nozzle, a 3D open impeller with full inducer, a parallel-wall vaneless diffuser and a collector. High-accuracy overall performance data were obtained for this compressor.

The experiments were carried out in a closed-loop centrifugal compressor test rig with the impeller running at a rotational Mach number u_2/a_o = 1.39. The impeller tip diameter was 0.516 m, its tip width 0.021 m and the impeller blade exit angle was 30 degrees from radial.

Assuming a linear relationship, the experimental data indicates a pressure ratio decrease of 0.77 percent, an efficiency loss of 0.31 points, an input head reduction of about 0.25 percent and an output head reduction of about 0.65 percent for each percent increase in clearance ratio. However, the data seems to indicate a non-linear effect showing stronger performance sensitivity at smaller clearances.

The test data are compared against a clearance loss model. Improved performance prediction is obtained by including the effect of clearance on impeller work input.

NOMENCLATURE

a - sonic speed of vapor
b - blade height
c - blade running clearance
Cr - clearance ratio c/b (calculated as axial tip clearance ratio c_2/b_2)
E - Euler input head coefficient
h - enthalpy
H_{in} - work input coefficient (see Equation (1))
H_{pol} - polytropic head coefficient (see Equation (2))
P - total pressure
Pr - total-to-total pressure ratio
Q - volumetric flow rate
rh - hub radius
rs - shroud radius
Re - Reynolds number
T - total temperature
u - wheel speed
vtan - tangential velocity
vmer - meridional velocity
V - specific volume
Z - number of blades

Greek
β - blade angle from radial
Δq_{cl} - clearance loss coefficient
η - efficiency
λ - distortion factor
ρ - density
ϕ - flow coefficient
σ - slip factor

Subscripts
$_0$ - @ compressor inlet
$_1$ - @ impeller inlet
$_2$ - @ impeller exit
$_3$ - @ diffuser exit

INTRODUCTION

Centrifugal compressor impellers may be open or shrouded (see Figure 1). The open impeller lacks the second bounding surface (shroud) connecting the tip edges of the impeller vanes. Both types of impellers are encountered in industrial centrifugal compressors. Low specific speed, two-dimensional centrifugal impellers with predominantly radial inlet flow are normally shrouded while high specific speed centrifugal impellers with full inducers (axial inlet flow) are often open. The open impeller has a small amount of fluid leaking over the edges of the blades. Tight running clearances are desirable to minimize the tip clearance leakage. The shrouded impeller has flow leaking back from impeller discharge to suction through the space between the stationary and rotating shroud. A labyrinth seal is normally applied to limit the amount of recirculating flow.

Presented at the Gas Turbine and Aeroengine Congress
Amsterdam, The Netherlands—June 6-9, 1988

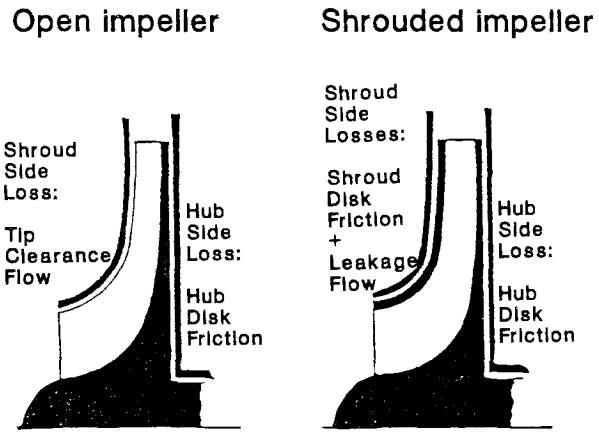

Figure 1. Open and shrouded centrifugal compressor impeller.

General statements about about efficiency and range advantages of the use of a shrouded versus an unshrouded impeller for a certain compressor application are difficult to make. Much depends on compressor design details such as the running clearance of an unshrouded impeller, the tightness of the front seal of a shrouded impeller and the surface roughness of casing and shroud cover. Harada (1985) tested the shrouded and open version of an identical impeller and found slightly better efficiencies and operating range for the open impeller. However, increasing the clearance of the open impeller or reducing the seal leakage flow of the shrouded impeller could easily have changed the conclusion in favor of the shrouded impeller.

The channel flow friction loss along the hub and the pressure and suction side blade surfaces can be assumed equal for both the shrouded and the unshrouded impeller. For the shrouded impeller, the channel flow friction loss occurs along the rotating shroud surface and is therefore proportional to the square of the relative fluid velocity along the shroud, while for the open impeller the channel flow friction loss occurs along the stationary shroud surface and is thus proportional to the square of the absolute fluid velocity along the shroud.

The flow leakage loss of the unshrouded impeller is due to leakage of fluid through the clearance between the stationary shroud and the tip of the impeller blades from pressure to suction side. Besides the loss in total pressure of the leaking fluid itself during passage through the clearance, this leakage fluid has the potential to disturb the internal flow characteristics of the bladed channel it is entering, since it moves in a direction opposite to secondary flow in the shroud boundary layer where the Coriolis force moves the low momentum boundary layer fluid from pressure to suction side in the channel. As is illustrated in Figure 2, these two opposite streams of low momentum fluid will cause a wake covering part of the core flow area of the channel.

Shrouded impellers do not suffer from this performance degradation due to leakage of fluid through the running clearance between the impeller and the stationary shroud surface. However, they encounter two other loss mechanisms: disk friction loss between casing and rotating shroud and leakage loss of impeller discharge fluid leaking back in the space between the rotating impeller shroud and the stationary casing and through the inlet labyrinth seal to the suction side of the impeller. Fairly reliable models have been known for a long time to quantify the disk friction (Daily and Nece, 1960) and labyrinth seal (Egli, 1935) losses. These correlations have successfully been implemented in overall centrifugal compressor performance analysis programs.

The effect of clearance of open impellers on compressor performance is less well understood. One of the reasons is that its effect can only be tested on a real compressor suffering from all other possible loss mechanisms at the same time. The effect can not be isolated as easily as the effect of for example disk friction and seal leakage. This means that specific aerodynamic characteristics such as impeller blade loading and overall internal flow diffusion level might have an important effect on the clearance loss.

There also exists a measurement problem. An accurate measurement of the running impeller clearance is difficult to make. The clearance is only a fraction of the blade height. For small diameter impellers, impeller clearances of a few hundreds of a mm are not uncommon. Also, the running clearance is to be measured as opposed to the cold clearance before machine start-up. Axial impeller thrust forces and temperature effects cause the running clearance to be different. Rubbing probes (Klassen et al. 1977 and Schumann et al. 1987) and eddy current proximity probes (Harada 1985) have been used to measure running clearances. As an extra complication it will be found that, in general, tip clearance is not circumferentially uniform due to finite precision of the various components. This deviation can show up when very tight clearances have to be achieved.

In most experiments clearance variation is realized by shimming the impeller axially away from the shroud. This will increase the axial component of the clearance and the vaneless diffuser width. The pure radial clearance at the inducer section of the impeller will not be influenced by the increase in axial clearance.

A survey of the experimental data presented in the literature on the effect of clearance on centrifugal compressor performance shows a large amount of scatter.

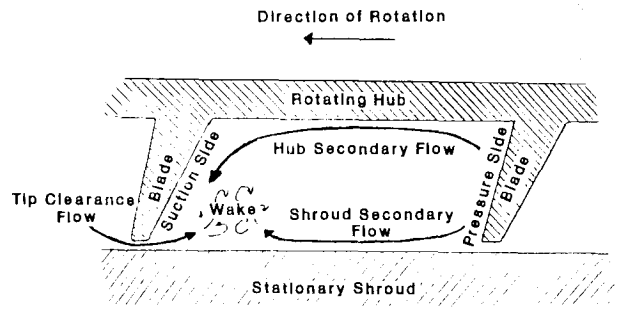

Figure 2. Secondary flow pattern in the radial part of a centrifugal compressor showing the interception of the tip clearance flow by the secondary flow in the shroud boundary layer.

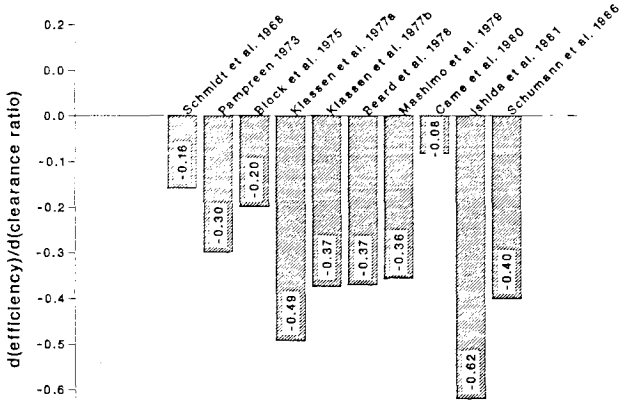

Figure 3. Summary of the literature on centrifugal compressor axial clearance tests showing variation in reported overall efficiency dependence on clearance ratio.

Figure 3 summarizes the experimentally reported sensitivity of centrifugal compressor efficiency to a change in tip clearance ratio. Table 1 summarizes the main characteristics of the centrifugal compressors used in the clearance test experiments compared in Figure 3. This data base of published tip clearance experiments was not considered consistent enough to make a reliable prediction of the effect of tip clearance on compressor performance. Therefore, an experimental program was initiated to study the effect of tip clearance of an unshrouded impeller on overall compressor performance.

All reported clearance studies, with the exception of Block and Runstadler (1975), were performed with air compressors. The current experiment used a refrigerant 11 compressor. The advantage of the use of refrigerant 11 from an experimental point of view is its low sonic speed and its low ratio of specific heats. As a result comparable pressure ratio's can be obtained at a fraction of the wheel speed needed for an air compressor and with a substantially smaller temperature rise. This significantly reduces the differences between cold and running clearances as observed in air compressors. It also allows the testing of larger diameter impellers at moderate tip speeds with modest input power requirements. As can be seen from Table 1, our compressor has a substantially larger impeller diameter than any of the compressors tested previously.

TABLE 1. Pressure ratio, impeller diameter and clearance ratio range of centrifugal compressors tested in previous clearance experiments.

Reference	Pressure Ratio (-)	Impeller Diameter (m)	Clearance Ratio (-)
Schmidt e.a. 1968	3.4	0.355	0.035-0.140
Pampreen 1973	5.0	0.100	0.013-0.100
Block e.a. 1975	9.0	0.120	0.050-0.150
Klassen e.a. 1977a	6.0	0.161	0.039-0.113
Klassen e.a. 1977b	6.0	0.137	0.076-0.207
Beard e.a. 1978	3.6	0.246	0.022-0.065
Mashimo e.a. 1979	2.0	0.154	0.013-0.125
Came e.a. 1980	6.5	0.275	0.047-0.215
Ishida e.a. 1981	1.2	0.255	0.007-0.211
Schumann e.a. 1986	5.5	0.208	0.023-0.153
This study	3.4	0.516	0.032-0.139

EXPERIMENTAL SET-UP

Compressor Configuration

A compressor was build and tested consisting of a converging inlet nozzle, an open centrifugal impeller with full inducer, a parallel-wall vaneless diffuser and a dump collector. The compressor was installed in a dedicated closed-loop centrifugal compressor test rig. Instead of the standard diffusing volute typically used in centrifugal compressors, a dump collector configuration was chosen for the test rig compressor in order to obtain circumferential uniform conditions which would facilitate the calibration and interpretation of local internal flow measurements. A cross-sectional drawing of the test compressor is shown in Figure 4. A converging inlet nozzle reduced the inlet cross sectional area from 0.292 to 0.073 m^2. The impeller inlet shroud diameter was 0.305 m, the inlet hub diameter was 0.076 m, the tip diameter was 0.516 m, the exit tip width 0.021 m and the impeller blade exit angle was 30 degrees from radial. The impeller was gear driven by a 500 HP electric motor and rotated at a speed of 7060 rpm. All compressor tests were conducted with refrigerant 11 resulting in an impeller tip Mach number $u_2/a_0 = 1.39$.

Instrumentation

The following pressures and temperatures were measured for overall performance evaluation. Four temperatures and two static pressures in the inlet plenum (at measurement station nr. 0, see Figure 4), four static and four total pressures at impeller inlet (measurement station nr. 1), four static pressures, four total pressures and four temperatures at diffuser discharge conditions (measurement station nr. 3) and two static pressures in the collector.

Precision thermistors with an accuracy better than $\pm$ 0.05 °C were used as temperature sensors.

Two separate diaphragm type variable capacitance pressure transducers with an accuracy within 0.1 % of reading were used for measurement of suction and discharge pressures. The suction and discharge pressure signals from the static pressure taps and the total Kiel probes, together with a high and low reference pressure, were multiplexed with a 12 channel Scanivalve wafer switch system to the pressure transducers. This procedure allows on-line pressure transducer calibration.

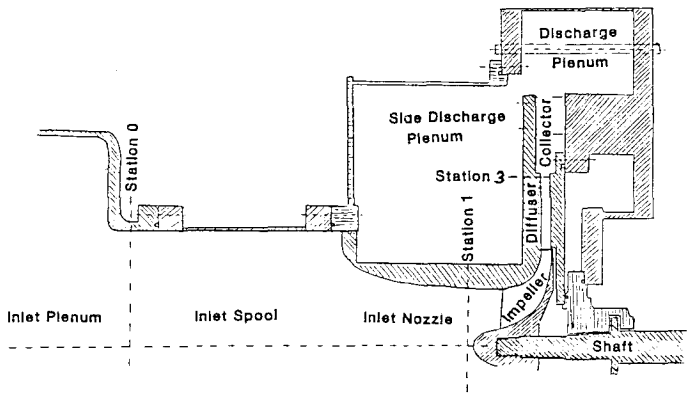

Figure 4. Cross section of centrifugal compressor build-up with inlet and discharge configuration and definition of location of measurement stations.

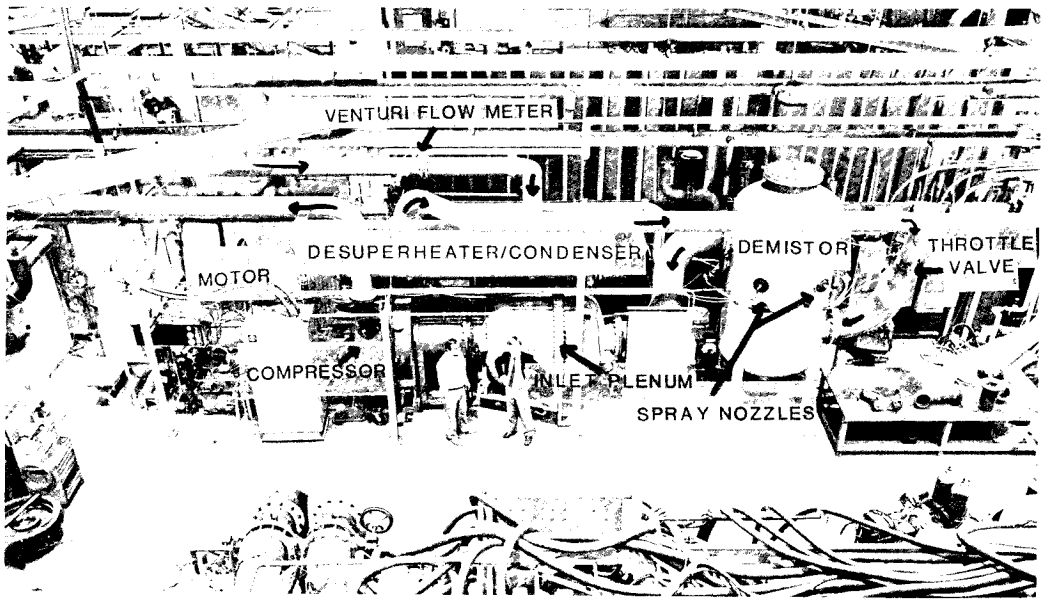

Figure 5. Picture of the 500 HP Centrifugal Compressor Test Facility.

Compressor mass flow rate was determined with an insert type venturi flow meter. The calculated venturi discharge coefficient was confirmed in a water loop calibration experiment where the predicted mass flow rate was compared against NBS calibrated orifice flow meters. The pressure drop over the venturi flowmeter and some additional loop resistances were measured with an accurate variable capacitance differential pressure transducer. This transducer is also on-line calibrated with two reference pressures.

Compressor Test Rig

The above described compressor build was tested in a dedicated centrifugal compressor test rig. Figure 5 shows a picture of this facility. The vapor leaving the compressor passes after a few 90 degree bends through a long straight section (20 pipe diameters long) before going through the venturi flow meter. The flow subsequently enters a desuperheater/condenser where the heat of the compression process is taken out of the vapor. Under normal operating conditions about 10% of the vapor will condense during this heat exchange process. The condensed liquid is collected from the bottom of the desuperheater/condenser. After passage through a subcooler it is pumped to the injection nozzles in the demistor. The bulk of the mass flow leaves the desuperheater/condenser from the top as saturated vapor and is expanded over a throttle valve to suction pressure level. The resulting low-pressure vapor flow enters a so-called demistor where its temperature is reduced by flash evaporization of the liquid from the subcooler which is injected through a set of spray nozzles. Thermodynamic equilibrium of the flow at suction temperature conditions is established in the demistor by giving the flow ample time for mixing the vapor and liquid phases. The flow leaving the demistor enters an inlet plenum where uniform, swirl-free inlet flow conditions are created by a set of wire screens and honeycomb meshes. This well-conditioned flow then enters the compressor where its pressure and temperature are raised again.

Loop control

Conditions in the test rig are set by fixing discharge pressure, suction pressure and suction temperature (see Figure 6). The discharge pressure is regulated by the cooling tower water flow rate going through the condenser, the suction pressure is controlled by the discharge pressure in combination with the pressure drop over the throttle valve (determined by the throttle valve position), and the suction temperature is controlled by the amount of liquid injected through the spray nozzles. Compressor discharge temperature and mass flow rate then determine compressor efficiency and capacity.

Refrigerant purity control

A large part of the centrifugal compressor test rig operates at sub-atmospheric pressures during test runs and the whole loop is slightly subatmospheric during shut-down. As a consequence, leak-tightness of the loop is a major concern, especially since the test rig does not have the full condenser of a standard chiller where all the vapor comes to rest and the non-condensable gases are trapped. Contamination of R11 with air will reduce compressor pressure ratio, work input coefficient and polytropic head coefficient and increase efficiency and stable operating range. Aerodynamically, it has the same effect as reducing the wheel speed. The purity of the refrigerant in the test rig is monitored by comparing saturation temperatures and pressures measured after the condenser/desuperheater with the theoretical refrigerant properties. For all tests reported the amount of air in the refrigerant was less than 0.6 percent on mass basis, eliminating any measurable

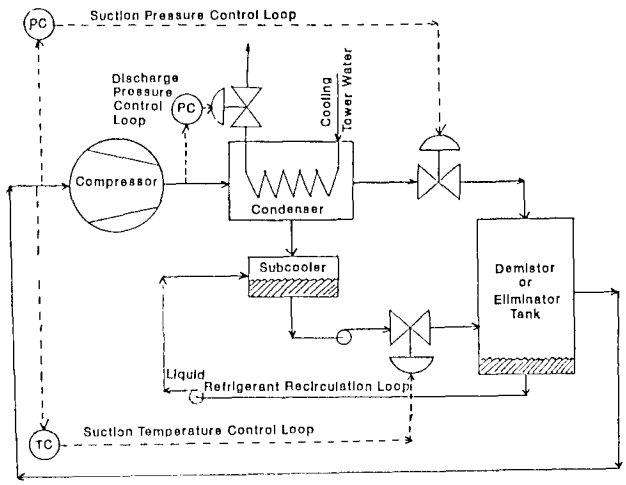

Figure 6. Schematic diagram of the centrifugal compressor test rig control system.

effect of refrigerant contamination on compressor performance.

Clearance control and clearance measurement

The axial impeller clearance is set by pulling the impeller against the axial thrust bearing and creating the design clearance of 0.75 mm by adding or removing shims between the stationary shroud and the machine casing. To measure the actual clearance under running conditions three polypropelene weld rods (a soft and non-brittle material that will be rubbed off by the blade tip of the impeller) were inserted through the shroud near the tip of the impeller 120 degrees apart. This measurement gave a circumferentially averaged running clearance of 0.68 mm, very close to the 0.75 mm design clearance. The three individual clearance measurements were 0.87, 0.82 and 0.35 mm indicating a slight misalignment between the shaft of the impeller and the stationary housing of about 0.15 degree. Larger clearances were realized by adding extra shims between the stationary shroud and the machine casing. As expected, the effect of the shaft misalignment on the circumferential clearance variation was relatively smaller for the larger clearances. The following four different clearance ratios Cr (circumferentially averaged clearance at impeller tip /impeller tip width) were realized: 3.18 (standard clearance), 6.35, 9.88 and 13.88 percent.

EXPERIMENTAL RESULTS

For each clearance ratio, compressor performance was determined for different flow rates going from compressor choke conditions (maximum flow rate) to compressor surge (minimum flow). Inlet temperature and inlet pressure were specified and experimentally realized by adjusting the control loop setpoints.

Definition of performance quantities

Compressor performance is determined from temperatures and pressures at inlet and outlet. The reported pressure ratio is the ratio between the averaged total pressure at the impeller inlet measured at station 1 (see Figure 4) and the averaged total pressure at the vaneless diffuser exit measured at station 3. For the calculation of efficiency, work input and polytropic head coefficient the average values of the compressor inlet and outlet temperatures, measured at stations 0 and 3 respectively, were used. The static pressures measured at the inlet plenum were equal to the total pressures measured at the impeller inlet (station 1). Therefore, aerodynamic losses between stations 0 and 1 can be neglected and the temperature measured at the inlet plenum can be used as the total temperature of the gas entering the compressor.

The compressor work input coefficient H_{in} is a dimensionless quantity defined as the increase in enthalpy between the compressor inlet and vaneless diffuser outlet condition divided by the square of the wheel tip speed $u_2 = \omega r_2$:

$$H_{in}(T_1,P_1,T_3,P_3) = \{h_3(T_3,P_3) - h_1(T_1,P_1)\}/u_2^2 \quad (1)$$

The polytropic head coefficient H_{pol} is the reversible work required to compress the gas in a polytropic process between the condition measured at impeller inlet (P_1,T_1) and the condition measured at the exit of the vaneless diffuser (P_3,T_3), divided by the square of the wheel tip speed:

$$H_{pol}(T_1,P_1,T_3,P_3) = \frac{1}{u_2^2} \int_{P_1,T_1}^{P_3,T_3} V(T,P)\, dP$$

$$\approx \frac{1}{u_2^2} \log\left(\frac{P_3}{P_1}\right) \left[\frac{P_3V_3 - P_1V_1}{\log\left(\frac{P_3V_3}{P_1V_1}\right)}\right] \quad (2)$$

The polytropic efficiency is then defined as the ratio of polytropic head coefficient over the work input coefficient.

$$\eta_{pol}(T_1,P_1,T_3,P_3) = \frac{H_{pol}}{H_{in}} \quad (3)$$

Complete overall compressor performance is defined when the pressure ratio and the efficiency are given as a function of flow rate. The purpose of introducing the two additional quantities of work input coefficient and polytropic head coefficient is to facilitate the understanding of the test data in terms of an overall compressor performance analysis model. These coefficients will be used in the section dealing with the theoretical calculations.

Sensitivity analysis

Based on the observation of the definitions of pressure ratio, polytropic efficiency, work input coefficient and polytropic head coefficient, the sensitivity of these four performance parameters on deviations in suction and discharge conditions can be established. Table 2 shows these sensitivities for deviations in pressures and temperatures at compressor design conditions. From this table is can be seen that pressure ratio and polytropic head coefficient depend strongly on suction and discharge pressure and to a much lesser extend on temperatures, while efficiency and input head coefficient depend strongly on temperatures and to a much lesser extend on pressures. It can also be seen that the accuracy of the temperature and pressure transducers (better than 0.05 °C and 0.1% respectively) is sufficient to guarantee an efficiency determination within 0.25 percent.

The method of determining efficiency from temperature and pressure measurements of compressor suction and

TABLE 2. Sensitivity of performance parameters on accuracy of inlet and discharge temperature and pressure measurement accuracy.

Deviation in temperature or pressure	Sensitivity of performance parameters ΔPr (%)	Δη (%)	ΔHin (%)	ΔHpol (%)
+ 1 % ΔP_1	-1.00	-0.87	+0.08	-0.80
+ 1 % ΔP_2	+1.00	+0.91	-0.11	+0.79
+ 1 °C ΔT_1	0.00	+2.45	-2.61	-0.18
+ 1 °C ΔT_2	0.00	-2.21	+2.41	+0.18

discharge gas assumes adiabatic compression. Heat losses during compression would lower the discharge gas temperature, which will result in lower input head and therefore higher efficiency when calculated from Equations (1) to (3). In order to eliminate the possibility of deviations in compressor performance due to differences in the amount of heat transfer, all clearance experiments were conducted at a fixed inlet temperature of 20 °C.

The accuracy of the test results is influenced by the precision and repeatability of the temperature and pressure sensors, the loop stability and the purity of the refrigerant. Loop stability turned out to become critical at conditions close to surge. It was found that before surge occurs, which is an audible effect accompanied by periodic drops in pressure and spikes in temperature, the overall process conditions start slightly fluctuating. Since it takes about ten minutes to collect all data from the temperature and pressure scanning systems, this process noise will reduce the accuracy of the data point.

For every data point a power balance check was made, comparing the impeller shaft input power (obtained from the motor input power corrected for motor efficiency and mechanical gear and bearing losses) with the compressor gas horse power. Data points with a power balance that deviated more than 1.5% were rejected. The majority of the rejected points occurred close to compressor surge conditions.

Test results

The compressor test data for each of the clearances are summarized in four plots (Figures 7 - 10). Figure 7 shows the compressor pressure ratio, Figure 8 the compressor polytropic efficiency, Figure 9 the work input coefficient and Figure 10 the polytropic head coefficient, all as a function of flow rate. Compressor performance curves which best approximate the experimental test data have been drawn in these figures to more clearly indicate the effect of clearance ratio on performance. Reading the values from these curves for the design flow rate (which is the peak efficiency point of the compressor at design clearance), the effect of clearance on performance has been determined. The results are plotted in Figures 11 to 14. Neglecting the data taken at clearance ratios

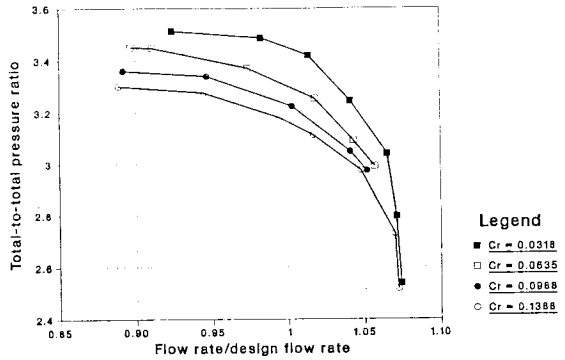

Figure 7. Total-to-total pressure ratio versus flow rate for different axial tip clearances.

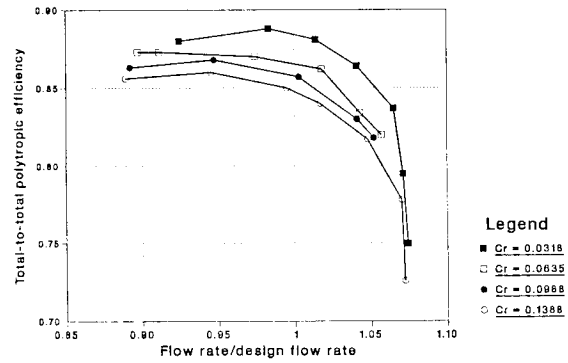

Figure 8. Total-to-total polytropic efficiency versus flow rate for different axial tip clearances.

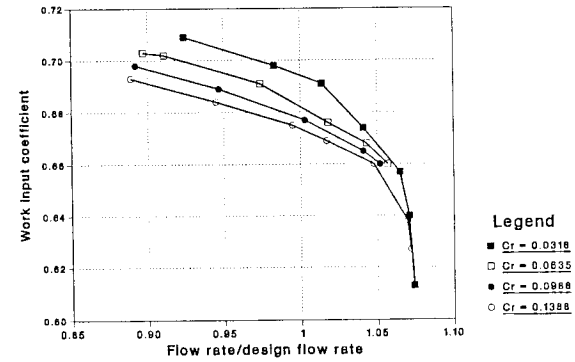

Figure 9. Work input coefficient versus flow rate for different axial tip clearances.

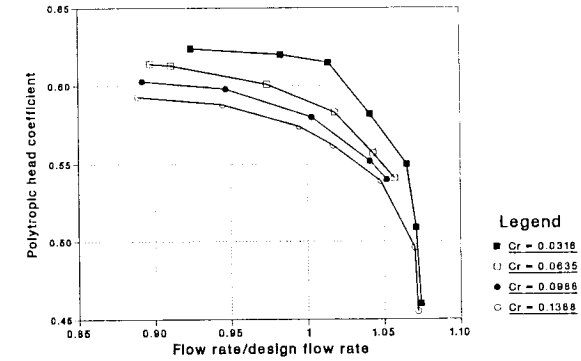

Figure 10. Polytropic head coefficient versus flow rate for different axial tip clearances.

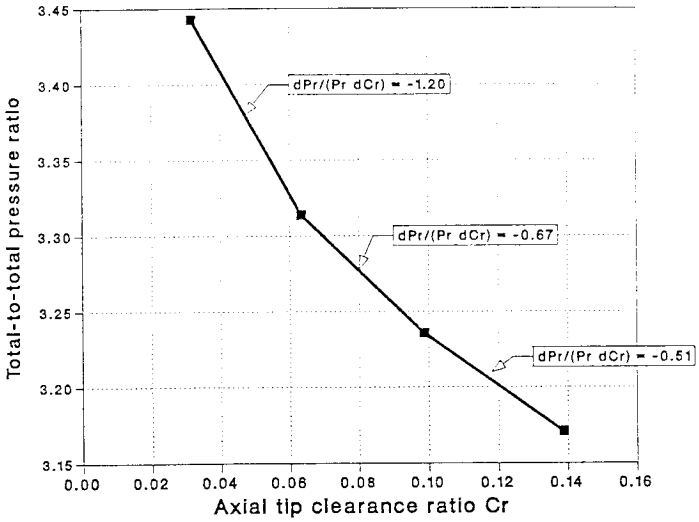

Figure 11. Pressure ratio as a function of axial tip clearance ratio at design conditions.

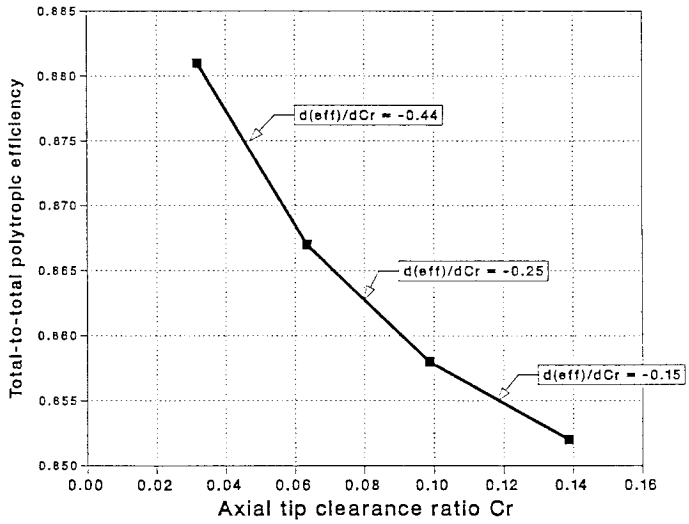

Figure 12. Polytropic efficiency as a function of axial tip clearance ratio at design conditions.

of 0.0635 and 0.0988 and assuming a linear relationship between clearance and performance, the experimental data taken at axial clearances of 0.0318 and 0.1388 indicates a pressure ratio decrease of about 0.77 percent, an efficiency loss of approximately 0.31 percent, an input head reduction of about 0.25 percent, and an output head reduction of about 0.65 percent for each percent increase in clearance ratio. However, it can be seen from Figures 9 to 12 that the effect of clearance variation on performance is initially (at lower clearances) more pronounced. This non-linear relationship between relative clearance and impeller performance could explain some of the discrepancies found in the literature.

5. THEORETICAL CALCULATIONS

Empirical clearance loss models

In the older centrifugal compressor literature, the efficiency drop and head reduction due to tip clearance of open impellers are simply given as a purely empirical and often linear function of some kind of clearance ratio. Eckert (1953) shows the following empirical relationships for efficiency drop as a function of clearance for centrifugal compressors:

$$\frac{\Delta\eta}{\eta} = -0.9\,\frac{2c}{b_1+b_2} \qquad (4)$$

head reduction as a function of clearance:

$$\frac{\Delta H}{H} = -0.9\,\frac{2c}{b_1+b_2} \qquad (5)$$

flow rate decrease as a function of clearance:

$$\frac{\Delta Q}{Q} = -0.5\,\frac{2c}{b_1+b_2} \qquad (6)$$

Schmidt-Theuner and Mattern (1968) summarized their experiments on the influence of clearance ratio on efficiency with a curve for efficiency deterioration due to increased clearance ratio which can be approximated by the following parabolic equation:

$$\Delta\eta = -0.23\,Cr + 0.46\,Cr^2 \qquad 0.035<Cr<0.140 \qquad (7)$$

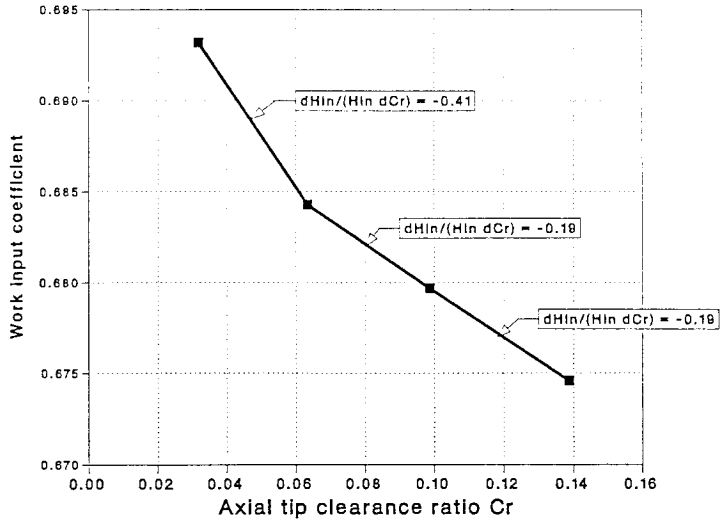

Figure 13. Work input coefficient as a function of tip clearance ratio at design conditions.

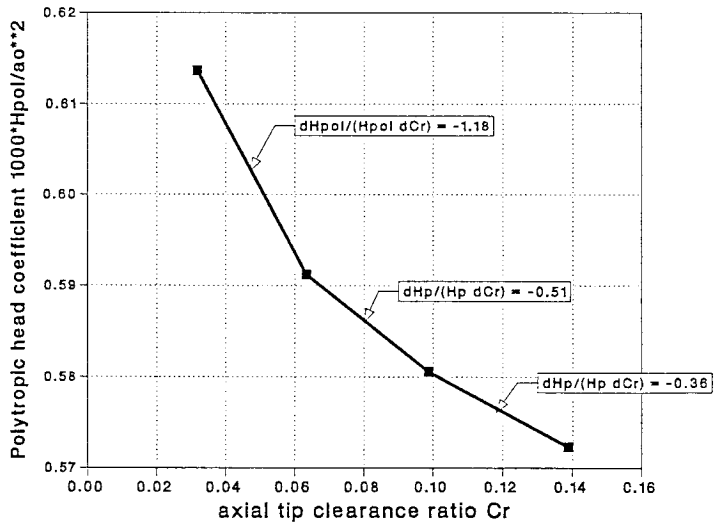

Figure 14. Polytropic head coefficient as a function of tip clearance ratio at design conditions.

It is interesting to note that, similar to our experimental results (see Figure 12), this equation shows the largest sensitivity of efficiency for clearance variation at the smallest clearance ratio.

Based on Pampreen's data (1973), Musgrave (1980) made the following linear correlation for the change in efficiency due to clearance:

$$\Delta\eta = -0.35\ Cr + 0.01 \qquad Cr > 0.03 \qquad (8a)$$

$$\Delta\eta = 0 \qquad Cr \leq 0.03 \qquad (8b)$$

Physical clearance loss model

Besides these purely empirical loss correlations, some clearance loss models based on first principles have been developed to predict the effect of clearance on centrifugal compressor performance. Jansen (1967) has postulated the following mechanism for clearance loss: the fluid through the clearance gap undergoes sudden contraction and subsequent expansion when it leaks from the high to the low pressure side of the blade and experiences a pressure loss equal to the blade loading. By assigning standard loss factors to the sudden contraction and sudden expansion processes, the following relationship for the clearance loss coefficient can be derived:

$$\Delta q_{cl} = \qquad (9)$$

$$0.6\ \left(\frac{c}{b_2}\right)\left(\frac{vtan_2}{u_2}\right)\sqrt{\frac{4\pi}{b_2 Z}\left[\frac{rs_1^2 - rh_1^2}{(r_2 - rs_1)(1+\rho_2/\rho_1)}\right]\left(\frac{vtan_2}{u_2}\right)\left(\frac{vmer_1}{u_2}\right)}$$

This clearance loss correlation has been adopted by a number of organizations in overall centrifugal compressor performance models, e.g. VandenBraembussche (1985).

Senoo and Ishida (1985,1986) developed a more detailed clearance loss model. Besides the pressure loss due to leakage through the clearance which is the physical phenomenon considered in the previous clearance loss models they identify an additional pressure loss for supporting the low-momentum fluid which originates from the clearance between the impeller and the shroud against the pressure gradient in the channels. There are two regions of low momentum fluid due to clearance. The first one is in the thin annular clearance space between the shroud and the impeller. The second one has a more complicated origin. It is caused by the interaction of the tip clearance leakage flow with the secondary flow in the impeller. The leakage flow through the tip clearance is namely intercepted by a secondary flow along the shroud which moves (opposite to the leakage flow) from the pressure side of a blade to the suction of the adjacent blade. When these two opposing low momentum flows meet, they move into the channel between the blades, form a wake and cause additional blockage. Figure 2 shows this secondary flow pattern in the radial part of a centrifugal impeller. As a result of this phenomenon the flow area of the impeller available for the inviscid core flow is reduced by the tip clearance and more power is needed from the core flow to support the stagnant flow in the wake areas against the adverse pressure gradients. Adding all three loss mechanisms, Senoo and Ishida arrive at a fairly complicated integral equation for the clearance loss coefficient. However, their clearance model is still only linearly dependent on the clearance ratio Cr while according to our experimental results the effect of clearance on performance is non-linear.

Comparison between clearance loss model and experiment

The effect of clearance on centrifugal compressor performance has been analyzed with an in-house centrifugal compressor performance analysis program. Only the impeller and the vaneless diffuser were modeled. The four performance characteristics studied in the experiments, namely impeller inlet to diffuser exit total-to-total efficiency, total-to-total pressure ratio, input head coefficient and polytropic head coefficient were calculated as a function of flow rate.

The in-house centrifugal compressor performance analysis program is capable of design as well as off-design performance calculations. It starts with the Euler input coefficient equation which predicts the ideal work input of the impeller:

$$E = (1 - \phi_2 \tan\beta_2) \qquad (10)$$

with ϕ_2 = impeller exit flow coefficient ($vmer_2/u_2$)
and β_2 = impeller discharge blade angle (from radial)

Equation (10) is an idealized situation since it assumes guidance of the flow by the impeller blades (no slip) and uniform flow profiles (no distortion). In reality there is slip and flow distortion leading to the definition of the real work input coefficient H_{in} defined as

$$H_{in} = \sigma\ (1 - \lambda\ \phi_2 \tan\beta_2) \qquad (11)$$

with σ = slip factor
and λ = impeller exit distortion factor

The polytropic head follows from the work input coefficient by accounting for the various losses, such as skin friction, incidence, choking, disk friction etc.. Equation (9) was used as clearance loss correlation.

Initial performance calculations indicated a much smaller dependence of input head coefficient on clearance ratio than experimentally found. The trend was even opposite to the test data: higher input head was predicted for larger clearances. In the performance analysis model, the input head reduces on the one hand, since due to the loss in total pressure in the impeller due to clearance (modeled by equation 9) the gas will leave the impeller at lower pressure, which means at lower density and therefore with a larger value of the discharge flow coefficient ϕ_2 and consequently a lower value of the work input coefficient H_{in}. On the other hand, however, the extra clearance will increase the passage width (b_2+c) at the tip of the impeller and therefore will reduce the impeller exit meridional velocity $vmer_2$ and therefore the impeller exit flow coefficient ϕ_2. Calculations indicated that for our specific impeller these two effects almost cancel each other, with the latter effect being slightly larger, resulting in a small increase in input head for larger clearance ratio's, opposite to the experimental findings.

This apparent contradiction between theory and experiment forced us to reconsider the definition of tip width for calculating the work input coefficient. Due to shear forces the impeller does work on the fluid between the impeller blade tip and the stationary shroud. However, it is questionable if this work can be treated the same way as the work done on the fluid in between the blades of the impeller, which is the underlying assumption when the passage width is used

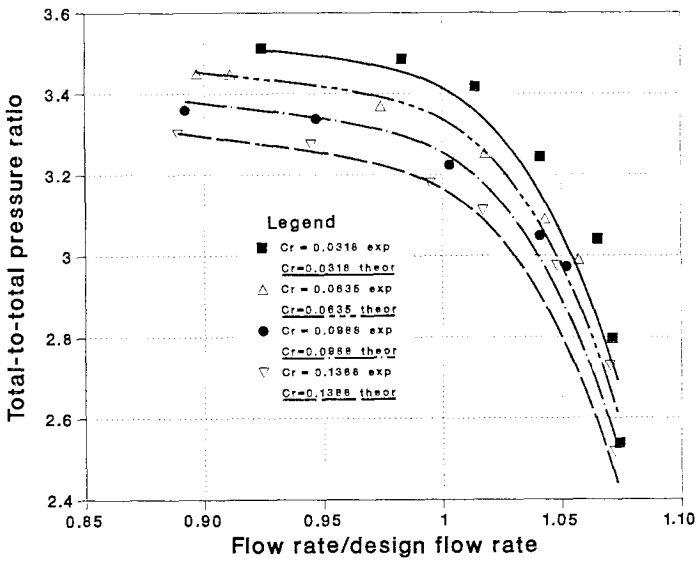

Figure 15. Experimental results and theoretical calculations of pressure ratio versus flow rate for different clearances.

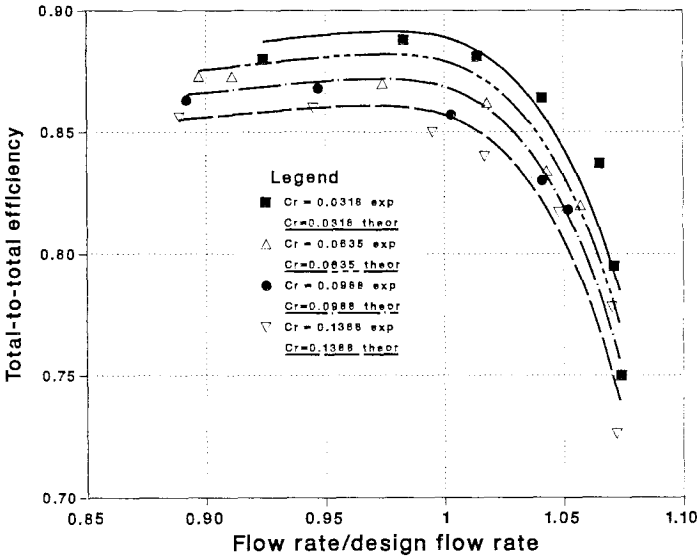

Figure 16. Experimental results and theoretical calculations of polytropic efficiency versus flow rate for different clearances.

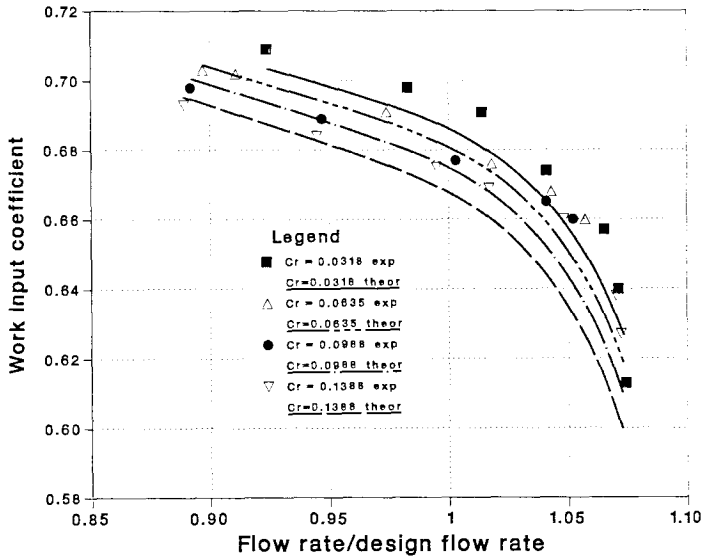

Figure 17. Experimental results and theoretical calculations of work input coefficient versus flow rate for different clearances.

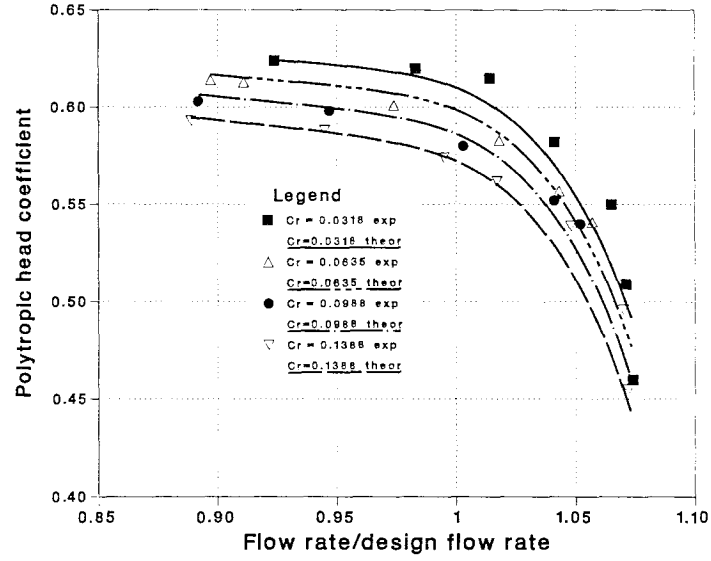

Figure 18. Experimental results and theoretical calculations of polytropic head coefficient versus flow rate for different clearances.

for the calculation of ϕ_2. It seems more reasonable to assume that the impeller does only partially work on the fluid between the impeller and the shroud. An good prediction of the input head coefficient as function of clearance was obtained when the effective impeller exit blade passage width was taken equal to the height of the impeller blade plus half the clearance. This approach, which means that the impeller does work on half of the fluid in the open space, seems very reasonable from a physical point of view.

With this modification of the modeling of the input head coefficient equation and using Equation (9) for the clearance loss, a fairly good prediction of the clearance tests could be obtained with our centrifugal compressor performance analysis program as illustrated by Figures 15 to 18. Obviously, the nonlinear effect of stronger performance sensitivity at smaller clearances can not be predicted by a linear loss correlation.

CONCLUSIONS

The axial clearance between the tip of the blades of an unshrouded impeller and its stationary shroud has been varied to study its effect on overall compressor performance.

Assuming a linear relationship, the experimental data indicates a pressure ratio decrease of 0.77 percent, an efficiency loss of 0.31 points, an input head reduction of about 0.25 percent and an output head reduction of about 0.65 percent for each percent increase in clearance ratio.

The data indicates a non-linear effect showing stronger performance sensitivity at smaller clearances.

Stable operating range was not markedly influenced by the additional clearance. A very small increase in stable operating range was observed.

An effort was made to predict the test results with an overall performance model. The effect of clearance on impeller work input was found to be critical. It could only be predicted correctly when in the calculation of the impeller exit flow coefficient the impeller tip cross sectional gas passage area was calculated from the blade height plus half the clearance.

REFERENCES

Beard, M.G., Pratt, C.M., and Timmis, P.H., 1978, "Recent Experience on Centrifugal Compressor for Small Gas Turbines", ASME 78-GT-193.

Block, J.A., and Runstadler Jr, P.W., 1975, "Effect of Specific Heat Ratio, Impeller Tip Running Clearance, and Compressor Insulation on High-Pressure-Ratio Centrifugal Compressor Modeling", Transactions of the ASME Journal of Fluids Engineering, Vol. 97, 174-179.

Van den Braembussche, R.V.D., 1985, "Design and Optimization of Centrifugal Compressors", Lecture given at the NATO Advanced Study Institute, Izmir, Turkey, September 1984 and published in Ucer, A.S., Stow P., and Hirsch, Ch., Ed.,"Thermodynamic and Fluid Mechanics of Turbomachinery", Martinus Nijhoff Publishers, Dordrecht, Vol.2, pp. 829-885.

Came, P.M., and Herbert, M.V., 1980, "Design and Experimental Performance of Some High Pressure Ratio Centrifugal Compressors", presented at the 55th (B) Specialists' Meeting of the Propulsion and Energetics Panel of AGARD, May 7-9, 1980, Brussels and published as Paper No. 15 in the AGARD Conference Proceedings No. 282 on Centrifugal Compressors, Flow Phenomena and Performance, Nov. 1980.

Daily, J.W. and Nece, R.E., 1960, "Chamber Dimension Effects of Induced Flow and Frictional Resistance of Enclosed Rotating Disks", Transactions of the ASME Journal of Basic Engineering, Vol 82, pp. 217-230.

Eckert, B., 1953, "Axialkompressoren und Radialkompressoren", Springer, Berlin.

Egli, A., 1935, "The Leakage of Steam through Labyrinth Glands", Transactions of the ASME Journal of Basic Engineering, Vol 57, pp.115-122.

Harada, H., 1985, "Performance Characteristics of Shrouded and Unshrouded Impellers of a Centrifugal Compressor", Transaction of the ASME Journal of Power Generation and Gas Turbines, Vol 107, pp 528-533.

Ishida, M., and Senoo, Y., 1981, "On the Pressure Loss Due to the Tip Clearance of Centrifugal Blowers", Transactions of the ASME Journal of Engineering for Power, Vol. 103, pp. 271-278.

Jansen, W., 1967, "A Method for Calculating the Flow in a Centrifugal Impeller when Entropy Gradients are present", Proceedings of the Royal Soc. Conference of the Institution of Mechanical Engineers on "Internal Aerodynamics", Cambridge, England, Paper 12, pp. 133-149.

Klassen, H.A., Wood, J.R., and Schumann, L.F., 1977a, "Experimental Performance of a 16.10-Centimeter-Tip-Diameter Sweptback Centrifugal Compressor Designed for a 6:1 Pressure Ratio", NASA Technical Memorandum X-3552.

Klassen, H.A., Wood, J.R., and Schumann, L.F., 1977b, "Experimental Performance of a 13.65-Centimeter-Tip-Diameter Tandem-Bladed Sweptback Centrifugal Compressor Designed for a Pressure Ratio of 6", NASA Technical Paper 1091.

Mashimo, T., Watanabe, I., and Ariga, I., 1979, "Effects of Fluid Leakage on Performance of a Centrifugal Compressor", Transactions of the ASME Journal of Engineering for Power, Vol. 101, pp. 337-342.

Musgrave, D.S., 1980, "The Prediction of Design and Off-Design Efficiency for Centrifugal Compressor Impellers", in Performance Prediction of Centrifugal Pumps and Compressors, pp. 185-189, presented at the 25th Annual International Gas Turbine Conference, New Orleans, Louisiana, March 9-13.

Pampreen, R.C., 1973, "Small Turbomachinery Compressor and Fan Aerodynamics", ASME Journal of Engineering for Power, Vol. 95, 251-256.

Schmidt-Theuner, P., and Mattern, J., 1968, "The effect of Reynolds number and Clearance in the centrifugal compressor of a turbocharger", The Brown Boveri Review, Vol 55, No 8, 453-456.

Schumann, L.F., Clark, D.A., and Wood, J.R., 1987, "Effect of Area Ratio on the Performance of a 5.5:1 Pressure Ratio Centrifugal Impeller", Transactions of the ASME Journal of Engineering for Power, Vol. 109, pp. 10-19.

Senoo, Y., and Ishida, M., 1986, "Pressure Loss Due to Tip Clearance of Impeller Blades in Centrifugal and Axial Blowers", Transactions of the ASME Journal of Engineering for Gas Turbines and Power, Vol. 108, 32-37.

Senoo, Y., and Ishida, M., 1987, "Deterioration of Compressor Performance Due to Tip Clearance of Centrifugal Impellers", Transactions of the ASME Journal of Turbomachinery, Vol. 109, 55-61.